J|A|C|S
ARTICLES
Published on Web 01/07/2003

Theoretical Investigation of the Apparently Irregular Behavior of Pt−Pt Nuclear Spin−Spin Coupling Constants

Jochen Autschbach,*,† Ciprian D. Igna, and Tom Ziegler‡

Contribution from the Department of Chemistry, University of Calgary, Calgary, Alberta, Canada T2N 1N4

Received July 30, 2002; E-mail: jochen.autschbach@chemie.uni-erlangen.de

Abstract: One-bond Pt−Pt nuclear spin−spin coupling constants J(Pt−Pt) for closely related dinuclear Pt complexes can differ by an order of magnitude without any obvious correlation with Pt−Pt distances. As representative examples, the spin−spin couplings of the dinuclear Pt^{I} complexes $[Pt_2(CO)_6]^{2+}$ (**1**) and $[Pt_2(CO)_2Cl_4]^{2-}$ (**2**) have been computationally studied with a recently developed relativistic density functional method. The experimental values are $^1J(^{195}Pt-^{195}Pt) = 5250$ Hz for **2** but 551 Hz for **1**. Many other examples are known in the literature. The experimental trends are well reproduced by the computations and can be explained based on the nature of the ligands that are coordinated to the Pt−Pt fragment. The difference for J(Pt−Pt) of an order of magnitude is caused by a sensitive interplay between the influence of different ligands on the Pt−Pt bond, and relativistic effects on metal−metal and metal−ligand bonds as well as on "atomic orbital contributions" to the nuclear spin−spin coupling constants. The results can be intuitively rationalized with the help of a simple qualitative molecular orbital diagram.

1. Introduction

One of the two most important observables of nuclear magnetic resonance (NMR) is the nuclear spin−spin coupling constant J(A−B). Of special interest are coupling constants between heavy atoms because they can be difficult to observe experimentally and hard to interpret and reproduce theoretically. Unlike the case of chemical shifts, theoretical predictions of coupling constants cannot benefit from effective cancellations of errors for separate calculations of a sample and the reference, hence their computation is comparatively demanding. Only recently the methodology for a reliable prediction of coupling constants for heavy nuclei based on first principles theory has become available because for their determination both a relativistic formalism and the inclusion of electron correlation is necessary.[1−5] Density functional theory is currently the method of choice for an investigation of properties of heavy metal complexes because it offers a reasonably accurate electronic structure for these systems, along with computational efficiency that is needed because of the many electrons to deal with. Researchers are now in the position to theoretically investigate problems regarding heavy atom NMR which could not yet be solved based on experimental data alone.

$J(^{195}Pt-^{195}Pt)$ coupling constants have been studied for a long time,[6−9] but they are not well understood. For chemically closely related complexes, variations in J(Pt−Pt) by an order of magnitude occur.[7,9] These variations do not correlate with distances between the Pt centers. Examples are $[\{Pt(CO)_3\}_2]^{2+}$, $[\{PtCl(CO)(PPh_3)\}_2]$, and $[\{Pt(CNCH_3)_3\}_2]^{2+}$, with small Pt−Pt coupling constants of 551, 760, and 507 Hz, respectively, and on the other hand $[\{PtCl_2(CO)\}_2]^{2-}$ and $[\{PtBr_2(CO)\}_2]^{2-}$, with large Pt−Pt coupling constants of 5250 and 4770 Hz, respectively. Other examples can be found, e.g., in ref 7. The Pt oxidation state is +I in all cases listed here. Further, it has been found that the Pt−C coupling constants do not differ much between the complexes, which also testifies to their chemical similarity. So far, no rational for the trends in these experimental data has been forthcoming. It is our aim here to report a computational analysis of J(Pt−Pt) for the complexes $[Pt_2(CO)_6]^{2+}$ (**1**) and $[Pt_2(CO)_2Cl_4]^{2-}$ (**2**) as representations for the groups of complexes with small and large J(Pt−Pt), respectively, in an attempt to reproduce and understand the difference. The Pt−Pt coupling constant of the less stable isomer **3** (see next page) of complex **2** is also studied for comparison.

In Section 2, we outline the computational details. In Section 3, the results of the calculations are compared to experiment. It will be shown that the experimental findings are reproduced by the computations, and that the interplay between the ligands influence and relativistic effects on the Pt−Pt bond in **1** and **2** is responsible for the seemingly irregular behavior of J(Pt−Pt). σ interaction of the Pt−Pt fragment with ligands causes a reduction of the Pt−Pt coupling constant and quenches its

* To whom correcpondence should be addressed.
† Present address: Lehrstuhl für Theoretische Chemie, Universität Erlangen, Egerlandstrasse 3, D-91058 Erlangen, Germany.
‡ Electronic mail: ziegler@ucalgary.ca

(1) Visscher, L.; Enevoldsen, T.; Saue, T.; Jensen, H. J. A.; Oddershede, J. *J. Comput. Chem.* **1999**, *20*, 1262−1273.
(2) Enevoldsen, T.; Visscher, L.; Saue, T.; Jensen, H. J. A.; Oddershede, J. *J. Chem. Phys.* **2000**, *112*, 3493−3498.
(3) Kirpekar, S.; Sauer, S. P. A. *Theor. Chem. Acc.* **1999**, *103*, 146−153.
(4) Autschbach, J.; Ziegler, T. *J. Chem. Phys.* **2000**, *113*, 936−947.
(5) Autschbach, J.; Ziegler, T. *J. Chem. Phys.* **2000**, *113*, 9410−9418.
(6) Pregosin, P. S. *Annu. Rep. NMR. Spectrosc.* **1986**, *17*, 285−349.
(7) Boag, N. M.; Browning, J.; Crocker, C.; Goggin, P. L.; Goodfellow, R. J.; Murray, M.; Spencer, J. L. *J. Chem. Res. (M)* **1978**, 2962−2990.
(8) Boag, N. M.; Goggin, P. L.; Goodfellow, R. J.; Herbert, I. R. *J. Chem. Soc., Dalton Trans.* **1983**, 1101−1107.
(9) Xu, Q.; Heaton, B. T.; Jacob, C.; Mogi, K.; Ichihashi, Y.; Souma, Y.; Kanamori, K.; Eguchi, T. *J. Am. Chem. Soc.* **2000**, *122*, 6862−6870.

10.1021/ja027931q CCC: $25.00

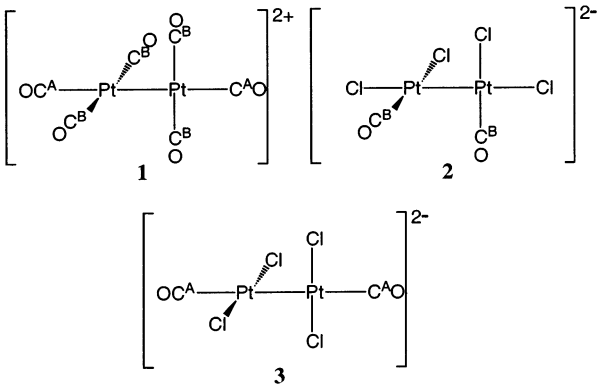

relativistic increase, in particular in the case of CO located trans to the other platinum. The results are further rationalized with the help of a simple molecular orbital diagram. Section 4 summarizes the results.

2. Methodology and Computational Details

All computations have been carried out with the Amsterdam Density functional (ADF) program package.[10−12] The computations employ our recently developed density functional method for the analytic calculation of nuclear spin−spin coupling constants[4,5] based on the relativistic zero-order regular approximation (ZORA).[13,14] The Vosko−Wilk−Nusair (VWN) local density functional[15] has been used throughout since it provides a reasonable accuracy for structures and spin−spin couplings of heavy metal complexes.[4,5,16−18] The coupling constants have been computed for the optimized geometries (scalar ZORA, ADF Basis ZORA/TZP,[12] 4f frozen core for Pt, 1s frozen core for C and O, 2p frozen core for Cl). We use the nonrelativistic terminology here for the ZORA relativistic analogues of the Fermi-contact (FC), spin-dipole (SD), paramagnetic orbital (OP), and the diamagnetic orbital (OD) terms on which the coupling constant calculations are based. All coupling constants are dominated by the scalar relativistic FC term, to which the present analysis is thus restricted. The OD term is completely negligible in all investigated coupling constants. The OP term was found to be nonnegligible, but typically less than 20% of the FC term in magnitude. Spin−orbit computations including the SD term have been carried out in order to ensure that they yield similar results and the same trends as the scalar relativistic calculations. Spin−orbit and SD contributions to the coupling constants are not negligible in the present cases, but small enough to justify a scalar relativistic treatment and thus a much simplified analysis of the FC term. We refer to refs 4, 5, 16, and 17 for further details on the computations of the spin−spin coupling constants and the all-electron basis sets employed for this purpose, as well as for benchmark data.

Table 1. Comparison of Computational (scalar ZORA, VWN functional) and Experimental $^{195}Pt-^{195}Pt$ Nuclear Spin−Spin Coupling Constants for **1** and **2**[*], in Hz[**]

		1	**2**
J(Pt−Pt)	calcd[f]	873.6	6397
	expt	550.9[a]	5250[b]
J(Pt−C^A)	calcd[f]	1632[c]/188.2[d]	
	expt	1281.5[a,c]/199.6[a,d]	
J(Pt−C^B)	calcd[f]	1817[c]/−34.81[d]	2492[c]/−55.35[d]
	expt	1595.7[a,c]/−26.2[a,d]	2000[b,c]/−48[b,d,e]

[*] Further data: $\delta(^{195}Pt)$: **2** with respect to **1** 710 ppm (spin−orbit: 610 ppm; expt.[a]: 582 ppm). Symmetry of optimized structures: D_{2d} for **1**, C_2 for **2**. R(Pt−Pt): **1** = 2.64 Å (expt.[a] 2.72 Å), **2** = 2.61 Å (expt.[b] 2.58 Å). R(Pt−C^A): **1** = 1.97 Å, R(Pt−C^B): **1** = 1.94 Å, **2** = 1.80 Å (expt.[a] average of R(Pt−C^A) and R(Pt−C^B) for **1** = 1.96 Å; crystal structure data[b] for **2** = 1.80 Å (mean value)). R(Pt−Cl): **2** = 2.43 Å(ax.)/2.33 Å(eq.) (expt.[b] averages: 2.40 Å(ax.)/2.34 Å(eq.)). [**] See Figure 1 for a comparison of relativistic and nonrelativistic theoretical data. [a] Ref 9, in concentrated H_2SO_4. R(Pt−Pt) and average value of R(Pt−C^A) and R(Pt−C^B) from EXAFS measurements in solution. [b] Ref 8, in CD_2Cl_2/CH_2Cl_2. R(Pt−Pt) from single-crystal X-ray diffraction, ref 21. [c] One-bond coupling ^1J. [d] Two-bond coupling ^2J. [e] Sign not determined experimentally. [f] Scalar ZORA including the FC, OP and OD term. Spin−orbit ZORA results further including the SD term: **1** = 1512./172.0 Hz for J(Pt−C^A), 1713./-30.72 Hz for J(Pt−C^B), 1062. Hz for J(Pt−Pt); **2** = 2446./-52.57 Hz for J(Pt−C^B), 7261 Hz for J(Pt−Pt).

3. Results and Discussion

Table 1 lists the computational results based on optimized geometries for the complexes **1** and **2**, in comparison with experimental data. Figure 1 illustrates the strong sensitivity of the results with respect to geometrical parameters. In light of this sensitivity, the theoretical results can be regarded as satisfactory since environmental effects (solvent, temperature) are not considered. For J(Pt−Pt) it can be expected that solvent effects will somewhat reduce its magnitude[19] in all cases, which would correct for its systematic overestimation in all computations when compared to experiment. Most important, the orders of magnitudes and the trends for the Pt−Pt and Pt−C couplings, and in particular the increase of J(Pt−Pt) by almost a factor of 10 from **1** to **2**, are well reproduced. The trend regarding the Pt−Pt coupling constants remains the same for the plotted range of Pt−Pt distances in Figure 1. This eliminates the possibility that external factors are responsible for the large difference in the Pt−Pt coupling constants, or that is caused by small differences in the Pt−Pt bond length.

For the following analysis, it is important to recall that "relativistic effects" play a major−often the leading−role in spin−spin coupling constants involving elements as heavy as Pt.[18,20] Very large coupling constants are frequently found for pairs of heavy nuclei that can often be attributed to relativistic effects only. Of equal importance for the present case is obviously the nature of the ligands that define the chemical environment, and "cross terms"—i.e., relativistic effects on the way the ligands bind to the metal.

It is therefore not surprising that relativistic effects have a great influence on the coupling between the two Pt nuclei in both complexes (Table 1 and Figure 1). As a consequence the

(10) Fonseca Guerra, C.; Visser, O.; Snijders, J. G.; te Velde, G.; Baerends, E. J. Parallelisation of the Amsterdam Density Functional program Program. In *Methods and Techniques for Computational Chemistry*; STEF: Cagliari, 1995.
(11) te Velde, G.; Bickelhaupt, F. M.; Baerends, E. J.; van Gisbergen, S. J. A.; Fonseca Guerra, C.; Snijders, J. G.; Ziegler, T. *J. Comput. Chem.* **2001**, *22*, 931−967.
(12) *Amsterdam Density Functional program*; Theoretical Chemistry, Vrije Universiteit: Amsterdam, URL: http://www.scm.com.
(13) van Lenthe, E.; Baerends, E. J.; Snijders, J. G. *J. Chem. Phys.* **1993**, *99*, 4597−4610.
(14) van Lenthe, E. The ZORA Equation. Thesis, Vrije Universiteit Amsterdam, Netherlands, 1996.
(15) Vosko, S. H.; Wilk, L.; Nusair, M. *Can. J. Phys.* **1989**, *58*, 1200.
(16) Autschbach, J.; Ziegler, T. *J. Am. Chem. Soc.* **2001**, *123*, 3341−3349.
(17) Autschbach, J.; Ziegler, T. *J. Am. Chem. Soc.* **2001**, *123*, 5320−5324.
(18) Autschbach, J.; Ziegler, T. Computation of NMR shieldings and Spin−spin Coupling Constants. In *Encyclopedia of Nuclear Magnetic Resonance*; Grant, D., Harris, R. K., Eds.; John Wiley & Sons: Chichester, 2002; Vol. Suppl., in press.
(19) Autschbach, J.; Igna, C. D.; Ziegler, T. Submitted for publication.
(20) Pyykkö, P. *Theor. Chem. Acc* **2000**, *103*, 214−216.

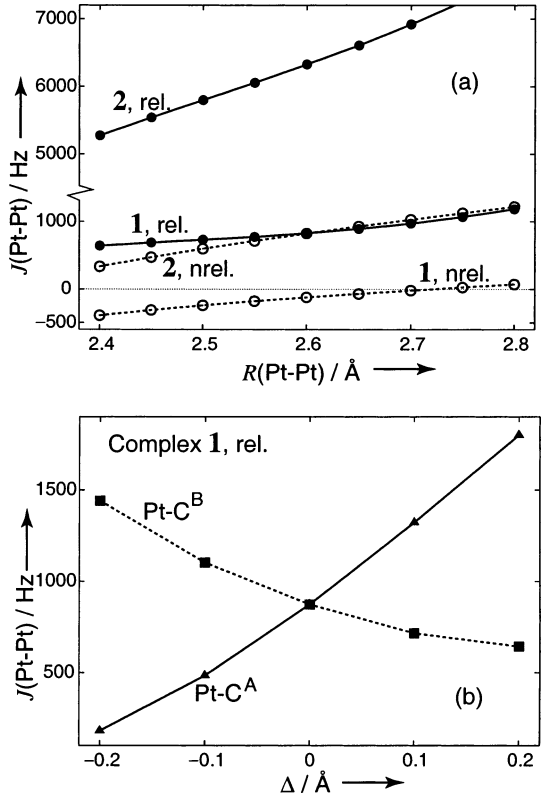

Figure 1. *J*(Pt−Pt) as a function of selected geometrical parameters. Figure (a): variation of the Pt−Pt distance in complex **1** and **2**, relativistic (filled markers) vs nonrelativistic values (open markers). Figure (b): variation of one of the Pt−C^A or Pt−C^B distances in complex **1**. Δ is the displacement from the optimized value.

magnitude of *J*(Pt−Pt) in **2** is not unexpected. It is stunning, however, that the corresponding value for **1** is so small. From the data in Table 1 and Figure 1, the following questions arise:

(1) why is the relativistic increase of *J*(Pt−Pt) for **1** so much smaller than for **2**, and

(2) why is *J*(Pt−Pt) already so small for **1** in the nonrelativistic calculations?

In case that the s-character of the Pt−Pt bond is determined mainly by the Pt 6s orbitals, based on a scaling of nonrelativistic atomic contributions to the Fermi-contact term of *J*(Pt−Pt)[22,23] one would expect a relativistic increase of *J*(Pt−Pt) by about an order of magnitude.[20] This appears to be the case for **2** but clearly not for **1**. An intermediate finding is, therefore, the following:

(1) it is the small magnitude of *J*(Pt−Pt) in **1** that needs an explanation,

(2) that the nature of the ligands is the major or only reason for the large variations of *J*(Pt−Pt),

(3) that the CO ligand tends to strongly reduce the Pt−Pt coupling constant already at the nonrelativistic limit, and

(4) that this reduction is even more pronounced in a relativistic calculation, with the effect that the already small *J*(Pt−Pt) in **1** increases relativistically by a much smaller amount as compared to the coupling in **2**.

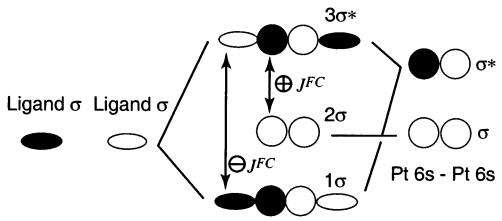

Figure 2. Qualitative symbolic MO diagram for the interaction of the 6s orbitals of the $[Pt-Pt]^{2+}$ fragment of **1** with the σ MOs of the axial ligands. The σ donation from the ligands into empty metal orbitals causes a negative $1\sigma-3\sigma^*$ contribution to *J*(Pt−Pt) and reduces the positive $2\sigma-3\sigma^*$ contribution relative to the free $[Pt-Pt]^{2+}$ fragment. The effect increases in magnitude the stronger the metal−ligand σ interaction is. See text for details.

It is well-known that for Pt, Au, Hg etc., relativistic effects enhance their capability to form strong σ bonds because of the 6s contraction/stabilization, the 5d expansion/destabilization and the concomitant increase of the $6s-5d_\sigma$ overlap.[24] This results here in competing effects regarding *J*(Pt−Pt) because on one hand the platinum atoms can form a stronger bond with each other. At the same time the σ interaction with the (axial, i.e., trans to the other Pt) CO ligands increases, which has a reducing effect on the s-character of the Pt−Pt bond. This is qualitatively outlined in Figure 2. The MO diagram also qualitatively explains why the metal−ligand interaction reduces the Pt−Pt coupling (see below). Regarding points 3 and 4 of the previous paragraph, the position of the CO ligand (axial, or equatorial i.e., trans to another ligand) is crucial. The D_{2d}-symmetric isomer **3** of complex **2** was found to be less stable by 155 kJ/mol in the computations. The calculated value for *J*(Pt−Pt) for **3** is −963.4 Hz. Obviously, the coordination to the Pt−Pt fragment by CO in axial position reduces *J*(Pt−Pt) most effectively, because **2** and **3** differ qualitatively only in the placement of the strongly (CO) and less strongly (Cl^-) interacting ligands in axial or equatorial position. (Clearly, he different nature of the equatorial ligands, when comparing **1** with **3**, is also of high importance for quantitative purposes, but for the sake of clarity not considered here for the qualitative aspects of the discussion.) It is also the Pt−C^A coupling that is very sensitive toward variations of the Pt−Pt distance, whereas the other Pt−C couplings do not change as much. This provides further evidence that the features of the Pt−Pt bond and of the axial Pt−C bonds are very strongly coupled.

It is possible with our program to decompose the coupling constant into contributions from pairs of occupied and virtual MOs, or, as we have newly implemented, from pairs of localized orbitals or orbitals of the constituting fragments of the molecule (here: Pt, Cl, and CO. See the appendix for details). The latter analysis for **1** in the relativistic case shows large negative contributions from pairs of Pt 5s and 6s orbitals, and the 5σ orbitals from the axial CO ligands, respectively, to *J*(Pt−Pt). In comparison, the equatorial CO ligands contribute less to *J*(Pt−Pt). There is no evidence that the CO π orbitals indirectly participate in the Pt−Pt coupling constant. Further, the analysis shows large negative contributions from the Pt $5d_\sigma$, but not from the $5d_\pi$ orbitals. These results can be taken as an indication that π back-donation plays little or no role for *J*(Pt−Pt) in **1**. This is also supported by the computational results of ref 9.

(21) Modinos, A.; Woodward, P. *J. Chem. Soc., Dalton Trans.* **1975**, 1516−1520.
(22) Pyykkö, P.; Pajanne, E.; Inokuti, M. *Int. J. Quantum Chem.* **1973**, *7*, 785−806.
(23) Khandogin, J.; Ziegler, T. *J. Phys. Chem. A* **2000**, *104*, 113−120.
(24) Pyykkö, P. *Chem. Rev.* **1988**, *88*, 563−594.

A Mulliken analysis yields—in good agreement with ref 9—Pt 6s populations of 0.7 and 5d populations of 8.5 for **1**. The populations for **2** are 0.8 and 8.5, respectively. The charge on Pt is smaller than 0.1 in magnitude for both complexes. Even though the larger s-population (and the shorter Pt−Pt distance) for **2** supports the fact that *J*(Pt−Pt) for **2** is larger, we have previously found[17] that the total s-population of the metal is not necessarily a good indicator for a comparison of its coupling constants. How the atomic valence s orbitals contribute to the bond in question is rather important because they are responsible for the portion of the charge density at or very close to the nuclei that is "shared" by the two Pt atoms (in an orbital model) and that causes the Fermi-contact term. Figure 2 qualitatively shows the interaction between ligand σ MOs and the 6s orbitals of a hypothetical Pt_2^{2+} fragment. As is outlined in the appendix, the pair of the occupied ⊕⊕ combination of the Pt 6s orbitals (σ) and the unoccupied ⊕⊖ 6s−6s combination σ^* yields a positive Fermi-contact contribution to *J*(Pt−Pt) in eq 1. The same holds for the pair of 2σ and $3\sigma^*$ orbitals in Figure 2. σ donation from the axial ligands means that the antibonding ⊕⊖ 6s−6s orbital mixes with the ⊕⊖ linear combination of the ligand σ orbitals. This new occupied orbital (1σ in Figure 2) causes a *negative* contribution to *J*(Pt−Pt) because of the sign pattern of the Pt-6s combinations in 1σ and $3\sigma^*$.

To estimate the magnitude of the FC term of *J*(Pt−Pt) in a complex, relative to the bare Pt_2^{2+} fragment, it is necessary to consider a) the coefficients of Pt−Pt σ and σ^* in the 1σ, 2σ, and $3\sigma^*$ orbitals, and b) their orbital energies. The former influence the value of $\varphi_i\varphi_a$ close to or at the Pt nuclei (see Appendix), whereas the latter enter the coupling constant directly as $(\epsilon_i - \epsilon_a)^{-1}$ in eq 1. The size of the negative $1\sigma-3\sigma^*$ contribution to *J*(Pt−Pt) with respect to the strength of the metal−ligand interaction is not easy to predict. On one hand, increasing metal−ligand interaction enlarges the coefficient of the Pt−Pt ⊕⊕ σ orbital in 1σ, which would give rise to a larger negative contribution to *J*(Pt−Pt). On the other hand, the coefficient of the Pt−Pt ⊕⊖ σ^* orbital in $3\sigma^*$ becomes smaller, and the energy gap between 1σ and $3\sigma^*$ increases. According to eq 1, this reduces the magnitude of the negative term. In summary, the magnitude of the negative contribution from $1\sigma-3\sigma^*$ depends on the actual situation (orbital levels and strength of interaction), but it is certainly responsible for some reduction of an initially positive *J*(Pt−Pt). At the same time, the positive contribution due to $2\sigma-3\sigma^*$ is also reduced when the metal−ligand interaction is strong, because of the smaller coefficient of the Pt−Pt σ^* orbital in $3\sigma^*$ as well as the enlarged energy gap between 2σ and $3\sigma^*$. An increasing metal−ligand interaction is therefore guaranteed to decrease the positive $2\sigma-3\sigma^*$ contribution to *J*(Pt−Pt) relative to *J*(Pt−Pt) of the free Pt_2^{2+} fragment. This qualitatively explains the differences of the ligands influence on the Pt−Pt bond between complex **1** and **2**.

The situation is somewhat more complicated in the actual systems because the Pt 6s orbitals contribute to a larger number of orbitals in none of which the 6s coefficients clearly dominate. Therefore, there exist a larger number of MOs in which Pt-6s and ligand σ mixing causes positive and negative contributions to *J*(Pt−Pt). However, each of them can be qualitatively rationalized by Figure 2.

4. Summary

It is evident from the computational data, and from their analysis in terms of fragment orbitals, that the σ interaction with the CO ligands in particular in axial position is responsible for the reduction of *J*(Pt−Pt) in **1** as compared to **2**. Due to the more pronounced σ bonding capability of Pt in the relativistic case, the expected large magnitude of the Fermi-contact contribution to *J*(Pt−Pt) in complex **1** is to a large extent compensated by the increasing σ interaction with the axial CO ligands. The ligand influence in **2** is much weaker in comparison. Figure 2 illustrates these findings.

The qualitative aspects of this analysis should be generally applicable to nuclear spin−spin coupling constants of metal−metal bonded complexes since they do not rely on specific features the Pt−Pt bond. That is, the coupling constant for a bare metal−metal fragment will be reduced upon coordination of this fragment in particular in case of a strong metal−ligand σ interaction and in particular when the ligands are in trans position to the other metal. A respective study by us of Hg−Hg coupling constants is currently under way.[19] For heavy metal coupling constants, it is important to consider the interplay between relativistic effects and the ligands influence in order to rationalize the experimental results. In this context, relativistic effects represent a "magnifying glass" for the observation of the influence of the ligands on the metal−metal bond.

Appendix

The FC contribution to the nuclear spin−spin coupling constant is (also in the ZORA relativistic) Kohn−Sham density functional method calculated as

$$J^{FC}(A-B) = \sum_{i}^{occ}\sum_{a}^{virt}\langle\varphi_i|\hat{A}|\varphi_a\rangle(\epsilon_i - \epsilon_a)^{-1}\langle\varphi_a|\hat{B}|\varphi_i\rangle \quad (1)$$

where the sums run over the occupied φ_i and virtual φ_a molecular Kohn−Sham orbitals with energies ϵ. Similar formulas are obtained for the OP and the SD terms. The operators $\hat{A}$ and $\hat{B}$ describe the perturbations due to the FC (OP, SD) term at nucleus *A* and *B*, respectively.[4,5] For the FC case, neglecting first-order changes of the molecular potential due to the presence of nuclear spins, $\langle\varphi_i|\hat{A}$ or $\hat{B}|\varphi_a\rangle$ samples the values of the product $\varphi_i\varphi_a$ *at* or *very close to* nucleus *A* or *B*, respectively and is thus determined by the s-orbital contributions to the molecular orbitals. Because $(\epsilon_i - \epsilon_a)^{-1}$ is negative for Aufbau configurations, the value of $\varphi_i\varphi_a$ has to be of different sign at *A* and *B* in order to yield a positive *a*, *i*-contribution to J^{FC}(A−B). This allows for an easy identification of positive and negative contributions to J^{FC} in eq 1 based on the bonding/antibonding character of φ_i and φ_a with respect to *A* and *B*. Equation 1 has been frequently employed to interpret coupling constants. An example is ref 25, in which an analysis of Pt−P and Pt−Pt coupling constants, based on a variant[26] of eq 1 and the nonrelativistic extended Hückel model, is presented. We have previously employed eq 1 for an interpretation of solvent effects on coupling constants involving a heavy metal.[16,17]

Equation 1 can also be understood as a sum of "orbital expectation values" $\langle\varphi_i|\hat{X}_i|\varphi_i\rangle$ of the perturbation operators $\hat{X}_i = \sum_a|\hat{A}|\varphi_a\rangle(\epsilon_i - \epsilon_a)^{-1}\langle\varphi_a|\hat{B}|$. The φ_i can be represented in a

(25) Koie, Y.; Shinoda, S.; Saito, Y. *Inorg. Chem.* **1981**, *20*, 4408−4413.
(26) Pople, J. A.; Santry, D. P. *Mol. Phys.* **1964**, *8*, 1.

different basis (e.g., fragment- or localized orbitals) λ_μ, with $\varphi_i = \sum_\mu \lambda_\mu C_{\mu i}$. The coupling constant is then given in terms of contributions from μ,ν-pairs of λ's and perturbation operators $\hat{Y}_{\mu\nu} = \sum_i C^*_{\mu i} C_{\nu i} \hat{X}_i$ as

$$J^{FC}(A-B) = \sum_\mu \sum_\nu \langle \lambda_\mu | \hat{Y}_{\mu\nu} | \lambda_\nu \rangle \qquad (2)$$

which can facilitate the interpretation of the result in particular when the λ-basis is localized and/or nonorthogonal. For the present case, we have analyzed the FC term of J(Pt−Pt) in terms of contributions in eq 2 from Pt atomic orbitals and the molecular orbitals of the axial and equatorial CO ligands.

Acknowledgment. This work has received financial support from the National Science and Engineering Research Council of Canada (NSERC). We are grateful to Prof. B. T. Heaton who has drawn our attention to the problem of Pt−Pt coupling constants.

Supporting Information Available: Optimized geometries for the three complexes (ASCII). This material is available free of charge via the Internet at http://pubs.acs.org.

JA027931Q